Ocean Engineering 39 (2012) 43–52

Contents lists available at SciVerse ScienceDirect

Ocean Engineering

journal homepage: www.elsevier.com/locate/oceaneng

An integrated multi-sensor data fusion algorithm and autopilot implementation in an uninhabited surface craft

Wasif Naeem [a,*], Robert Sutton [b], Tao Xu [c]

[a] School of Electronics, Electrical Engineering and Computer Science, Queen's University Belfast, Belfast BT9 5AH, UK
[b] School of Marine Science and Engineering, University of Plymouth, Plymouth PL4 8AA, UK
[c] School of Electrical Engineering and Automation, Tianjin University,Tianjin, China

ARTICLE INFO

Article history:
Received 25 May 2011
Accepted 10 November 2011
Editor-in-Chief: A.I. Incecik
Available online 25 November 2011

Keywords:
Unmanned surface vehicles
Data fusion
Navigation
Guidance
Control and environmental monitoring

ABSTRACT

Unmanned surface vehicles (USVs) are able to accomplish difficult and challenging tasks both in civilian and defence sectors without endangering human lives. Their ability to work round the clock makes them well-suited for matters that demand immediate attention. These issues include but not limited to mines countermeasures, measuring the extent of an oil spill and locating the source of a chemical discharge. A number of USV programmes have emerged in the last decade for a variety of aforementioned purposes. *Springer* USV is one such research project highlighted in this paper. The intention herein is to report results emanating from data acquired from experiments on the *Springer* vessel whilst testing its advanced navigation, guidance and control (NGC) subsystems. The algorithms developed for these systems are based on soft-computing methodologies. A novel form of data fusion navigation algorithm has been developed and integrated with a modified optimal controller. Experimental results are presented and analysed for various scenarios including single and multiple waypoints tracking and fixed and time-varying reference bearings. It is demonstrated that the proposed NGC system provides promising results despite the presence of modelling uncertainty and external disturbances.

1. Introduction

As the world is warming up, measures are being taken by the governments as well as organisations to reduce the effect of individual's activities on the environment. Purifying the surroundings is also a vital element in the ecological cleanup. Issues such as oil spills, such as the one recently caused by the explosion of deepwater horizon oil rig in the Gulf of Mexico (Petroleum, 2010), and water contamination, due to irresponsibly dumping hazardous waste in rivers and seas, are crucial areas demanding immediate attention. These have prompted the global community to act and devise solutions for such problems. One such project presented in this paper is the unmanned surface vehicle (USV) called *Springer* (see Fig. 1), funded by the Engineering and Physical Sciences Research Council (EPSRC), UK, which has been specifically designed to tackle the aforementioned problems.

In general, autonomous marine vehicles (AMVs), underwater and surface alike, have gained a widespread popularity among the marine research community in the last decade. They are being utilised in a number of application areas such as subsea pipeline surveying, surveillance missions, mines clearing operations, oil exploration to name a few. For instance, the ever popular *REMUS* AMV (Jordan, 2008) produced by Hydroid has been used for mines clearing operations in the Iraqi conflict of 2003. Maridan (2008) AMVs are being deployed in diverse missions such as archaeology and surveying and harbour protection. For mapping applications, the *Delfim* vehicle (Pascoal et al., 2000) has been developed. The underwater versions of those AMVs are suitable for deep sea operations and covert missions, however, they are subject to error produced by the onboard dead reckoning navigation system. Hence they require regular surfacing in order to obtain a GPS fix. On the other hand, USVs do not suffer from such a constraint. Moreover, USVs are quite suitable for tasks such as shallow water surveying where SCUBA divers or special vessels containing a number of personnel have to be employed thus incurring high operational costs. In other literature, USVs in conjunction with underwater vehicles are reported to be used to study hydrothermal vent activity (Pascoal et al., 2000).

To operate such vehicles, a robust and reliable navigation, guidance and control (NGC) system is required that involve minimum or no human intervention. The navigation system provides information related to the vehicle and target (e.g. position, velocity, etc.), whereas the guidance system generates suitable trajectories to be followed by the vehicle. A robust control system will then pilot the vehicle as closely as possible

* Corresponding author. Tel.: +44 2890974066; fax: +44 2890677023.
E-mail addresses: w.naeem@qub.ac.uk (W. Naeem), r.sutton@plymouth.ac.uk (R. Sutton), tao.xu09@googlemail.com (T. Xu).

0029-8018/$ - see front matter © 2011 Elsevier Ltd. All rights reserved.
doi:10.1016/j.oceaneng.2011.11.001

Fig. 1. *Springer* USV during trials at Roadford Reservoir, Devon.

to the desired trajectory despite the presence of external disturbances and modelling errors. For the *Springer* USV, these requirements have led to the development of a fault tolerant navigation system using a fuzzy multi-sensor data fusion (MSDF) algorithm and integrated with advanced guidance and control strategies based on optimal control theory. The autopilots include a fuzzy logic based linear quadratic Gaussian (LQG) controller and a genetic algorithm based model predictive controller (GA-MPC). The performances of both controllers were compared for various mission scenarios. In addition, a standard LQG controller was incorporated and a comparison is made in terms of the amount of control effort and setpoint tracking. A number of research papers have been published by the authors regarding the hardware design and simulation analysis of *Springer* USV, see for example Naeem et al. (2008). This paper presents experimental results on the development of the *Springer* mainly based on NGC system trials carried out at Roadford Reservoir in Devon, UK. Hence the primary intent of this paper is to report the development, integration and testing of the fuzzy-MSDF navigation technique with the guidance and control system design on *Springer*. Experimental data suggests that the approach is technically viable and is able to produce promising results.

The organisation of the paper is as follows: Section 2 presents the development of *Springer* USV whereas its physical modelling is briefly outlined in Section 3. The guidance and control system design is presented in Section 4 followed by a description of fuzzy-based MSDF algorithm in Section 5. Section 6 outlines the experiment setting whereas the results are illustrated in Section 7. Lastly, Section 8 contains discussion and concluding remarks.

2. *Springer* USV

The *Springer* USV is a low cost research vessel which was mainly designed to carry out pollutant tracking and environmental monitoring operations. It is also useful as a test bed platform for carrying out scientific and academic research in areas such as environmental data gathering, sensor and instrumentation technology, control systems engineering and designing of alternative energy sources.

The catamaran-shaped vessel is approximately 4 m long and 2.3 m wide with a gross weight of approximately 600 kg. Launch and recovery operations are conveniently carried out from an available slipway by at least two personnel. The USV is powered

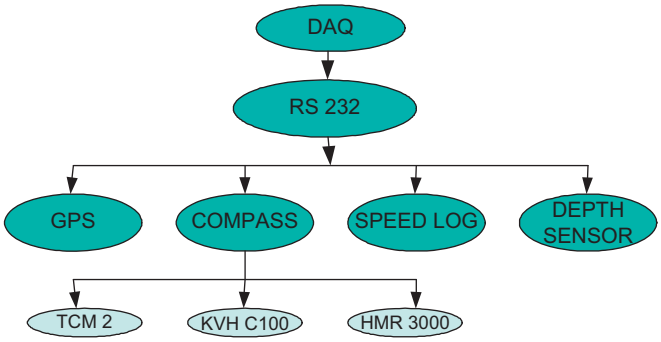

Fig. 2. *Springer* sensor suite.

by battery packs that are installed within both the hulls in addition to some onboard sensors and instrumentation. Pelicases are located within the bay areas between the two cross beams as evident from Fig. 1. These house the computers and the remaining onboard electronics and control circuitry. The wireless connectivity of the vehicle includes a WiFi router and a GPS unit mounted on a pole as depicted in Fig. 1. The introduction of a wireless network adds a useful remote intervention capability to the vessel in terms of providing external mission commands or simply resetting the system.

The sensor suite consists of three electronic compasses (TCM2, C100 and HMR1000), a GPS sensor, a Raymarine depth and velocity measurement unit and a YSI environmental monitoring sonde (see Fig. 2). The YSI sensor is capable of measuring several parameters such as turbidity, dissolved oxygen, pH to name a few and plays the key role in guiding the vehicle when tracking pollutants. To control the propulsion system, a RoboteQ controller (Roboteq, 2010) equipped with a built-in PID controller and leak sensor has been installed which accepts serial commands from the onboard PC and transmits to the actuators.

It can be observed that there is some sensor redundancy which is required for the MSDF algorithm in addition to providing fault tolerance capability. This will be further explained in Section 5. The NGC system for the *Springer* USV is designed to be robust, reliable and adaptable which allows seamless switching between automatic and manual control modes. In order to tune the NGC parameters, a dynamic model of the vehicle was developed using system identification (SI) techniques using measured input/output data by conducting experiments in a fresh water lake. A brief review of mathematical modelling and SI of *Springer* USV is carried out in the next section. For the interested reader, additional details of the modelling experiments are provided in Naeem et al. (2008).

3. Rigid body modelling and system identification

The generalised six degree of freedom (DOF) rigid body equations of motion of a vehicle are given in Fossen (1994) as

$$\mathbf{M}_{RB}\dot{v} + \mathbf{C}_{RB}(v)v = \boldsymbol{\tau}_{RB} \tag{1}$$

here $v = [u\ v\ w\ p\ q\ r]^T$ represents the linear and rotational motions of the rigid body in body-fixed coordinate system. $\mathbf{M}_{RB}$ is the rigid body inertia matrix satisfying

$$\mathbf{M}_{RB} = \mathbf{M}_{RB}^T > 0, \quad \dot{\mathbf{M}}_{RB} = 0$$

and the matrix $\mathbf{C}_{RB}$ correspond to the Coriolis and centripetal forces that can be parameterised to a skew symmetric matrix i.e.

$$\mathbf{C}_{RB}(v) = -\mathbf{C}_{RB}^T(v)$$

$\tau_{RB} = [X\ Y\ Z\ K\ M\ N]^T$ is a generalised vector of external forces and moments about the origin acting as an input to the system.

For a surface vehicle, the depth z and pitch θ variables are not applicable. Also, the roll ϕ variations were found to be negligible during the experiments and thus ignored. Expanding Eq. (1) with reference to the above statements results in the following four equations:

$$m[\dot{u}-vr-x_G(r^2)-y_G\dot{r}]=X \tag{2}$$

$$m[\dot{v}+ur-y_G(r^2+p^2)]=Y \tag{3}$$

$$\dot{p}I_x+prI_{xy}+my_G(vp)=K \tag{4}$$

$$rpI_x-\dot{p}I_{xy}-mx_G(vp)=M \tag{5}$$

See Appendix B for a Nomenclature. One can notice that by coinciding the centre of gravity with the origin, the above equations can be simplified further. Nevertheless, the intention was to model the dynamics of the vehicle and to gain insight into the system's behaviour. Evaluating the hydrodynamic coefficients through tank tests is a tedious and time consuming process. In addition, no such facility was available to conduct those tests. Hence it was deemed appropriate to model the vehicle using black box identification techniques such as SI. For this purpose, an umbilical was attached to the *Springer* whose other end was connected to a laptop on a support boat sending command and control signals. This proved to be a useful exercise as it allowed various onboard systems to be tested in addition to acquiring data for modelling purpose. In the following section, the steering dynamics of the vehicle is explained along with the analysis of the data collected for SI.

3.1. Steering dynamics

The *Springer* USV has a differential propulsion system which signifies that the manoeuvring is carried out using a set of thrusters. This incurs a simple dynamical model consisting of two inputs and a single output of interest as depicted in Fig. 3.

Where n_1 and n_2 are the revolution rates of the two propellers. Note that a difference in magnitude between n_1 and n_2 will result in a change in the direction of the vehicle. Hence, the common mode n_c and differential mode n_d thruster velocities can be written down as follows:

$$n_c=\frac{n_1+n_2}{2}$$

$$n_d=\frac{n_1-n_2}{2} \tag{6}$$

From the above equations, it can be observed that n_d is the only variable to be manipulated for controlling the vehicle's movement at a given velocity. This was made even simpler by incorporating the RoboteQ controller in the vessel which can be programmed to run either in separate (Fig. 3) or dual (Eq. (6)) mode. It can be noted that when $n_d=0$ i.e. $n_1=n_2$, the vessel traverse in a straight line.

In order to collect data for SI, the USV speed was held constant by maintaining n_c at 900 rpm which translates to a speed of approximately 3 kn. The desired manoeuvres were then obtained by transmitting n_d commands from the laptop through the umbilical. One of the data sets acquired for SI is presented in Fig. 4 which clearly shows the input–output pattern. The plot shows a section of the PRBS input and the corresponding heading output data. Note that there is a bias in the port side movement evident from the data which was partly blamed on irregular weight distribution within the hulls as well as misalignment of the two thrusters.[1]

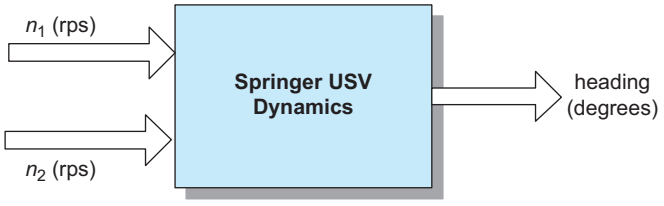

Fig. 3. Block diagram representation of a two-input USV.

SI techniques were then applied to the processed data and the following linear second-order single-input single-output state space model was obtained:

$$\mathbf{x}(k+1)=\mathbf{A}\mathbf{x}(k)+\mathbf{B}u(k)$$

$$y(k)=\mathbf{C}\mathbf{x}(k)+\mathbf{D}u(k) \tag{7}$$

where $u=n_d$ (rpm) is the differential input and $y=\psi$ (radians) is the output heading angle (controlled variable) of the USV. Note that the sway variable is ignored for simplicity. The state matrices are given by

$$\mathbf{A}=\begin{bmatrix}1.002 & 0\\ 0 & 0.9945\end{bmatrix},\quad \mathbf{B}=\begin{bmatrix}6.354\times10^{-6}\\ -4.699\times10^{-6}\end{bmatrix}$$

$$\mathbf{C}=[34.13\ \ 15.11]\quad\text{and}\quad \mathbf{D}=[0]$$

4. Guidance and control

An integrated guidance and control system forms a key component in effectively piloting the vehicle between the desired locations. The guidance system yields suitable trajectories whereas the autopilot keeps the vessel on the desired path whilst rejecting any disturbances. It may not be possible to avoid the external influence altogether such as winds and currents. In such events, the navigation system with the aid of additional sensors such as an anemometer, provides suitable information to the guidance system. This will then generate optimal paths to reach the target which may or may not be in a straight line. An obstacle detection and avoidance system is also imperative for a fully autonomous vehicle operation and should be integrated with the trajectory generation module. However, these systems are not yet installed on the vehicle and therefore will not be discussed any further. A hand-held anemometer with no feedback to the NGC system was however utilised to record wind measurements during the experiments.

Springer's guidance system utilises the simple LOS as well as waypoint following strategies. For mapping operations, the vehicle is guided through chemical signatures found in the water. This was explored in great detail in a review paper by Naeem et al. (2007). To control the vehicle, two modified optimal control techniques have been employed; fuzzy LQG and a GA-based MPC. These are briefly described in the following subsections.

4.1. Fuzzy LQG controller

LQG is an optimal control scheme which has been widely used in a variety of application areas. It is an amalgamation of a linear quadratic regulator (LQR) and a Kalman filter where the Kalman filter provide estimates of the unmeasured states to the LQR. Generally, four parameters are required to tune the LQG controller. Two of them being the process noise ($\mathbf{W}$) and measurement noise ($\mathbf{V}$) covariance matrices whereas the other two are the

[1] For safe launching and recovery operations, the thrusters are required to be manually pulled up each time causing this misalignment.

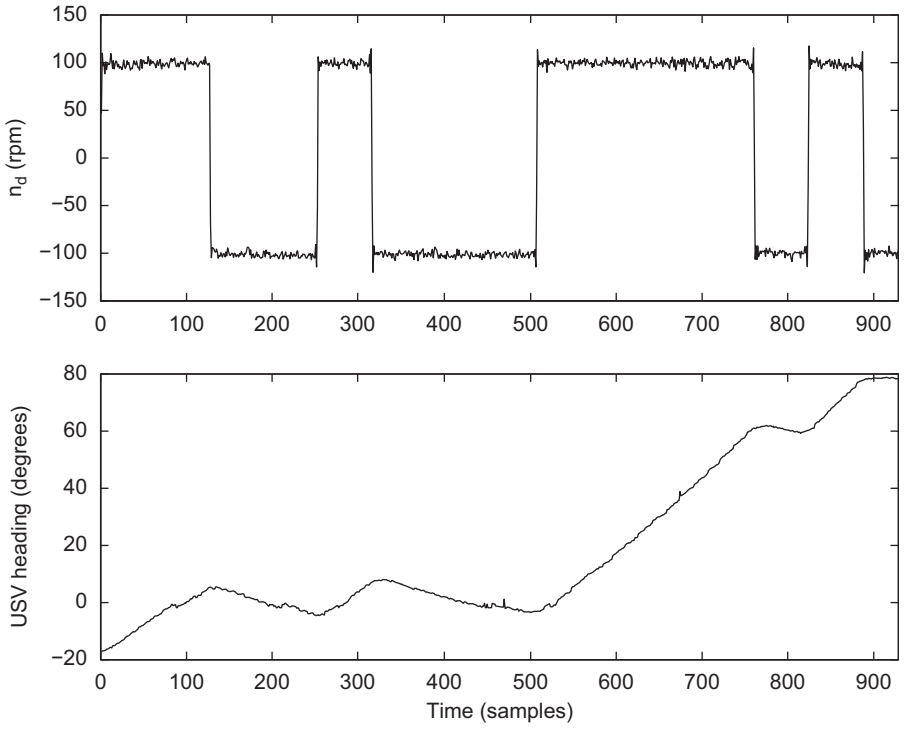

Fig. 4. A section of one of the experimental data set from trials conducted at Roadford Reservoir in Devon, UK.

state and control weighting (**Q** and **R**) matrices. The **Q** and **R** matrices are normally adjusted by observing the step response of the closed-loop system which should provide minimum settling time and zero steady state error among other specifications. The covariance matrices, on the other hand, are difficult to manipulate since they require ambient noise characteristics which is generally time-varying. Hence even a finely tuned controller could be subjected to a change in performance over a period of time. To rectify this problem, a modified LQG controller was proposed in Naeem et al. (2006) which uses fuzzy logic to tune the **V** matrix whilst maintaining **W**. In Shao et al. (1994), a similar approach is adopted to generate a LQG control law where the state and control weighting matrices are determined using a fuzzy logic adaptation mechanism. In other literature, the fuzzy logic is used to tune the **W** and **V** matrices of the Kalman filter (see for example Loebis et al., 2004b where the fuzzy membership functions are selected by a heuristic procedure). The Kalman filter in this particular instance is being used for a MSDF technique. Another enhancement to this approach was also proposed in Loebis et al. (2004a) which utilised multi-objective GAs to determine the fuzzy membership function parameters. The intention herein is to apply a heuristically tuned fuzzy inference system to adjust the covariance matrix and hence determine the Kalman gain. The resulting Kalman filter is then employed in an LQG framework.

This strategy has proved to generate reliable results irrespective of the environment in which the vehicle operates. The crux of this idea is a concept based on the innovation adaptive estimation (IAE) approach using a technique called covariance matching (Mehra, 1970). In this scheme, the theoretical ($S(k)$) and measured covariances ($\hat{C}_{Inn}(k)$) are determined and the difference in their magnitudes, $\delta(k)$, is used to alter the covariance matrices, $I_{nn}(k)$ being the innovation sequence given by the difference between the real measurement $z(k)$, received by the filter and its estimated value, $\hat{z}(k)$:

$$I_{nn}(k) = z(k) - \hat{z}(k) \tag{8}$$

$$\hat{C}_{Inn}(k) = \frac{1}{H}\sum_{j=j_0}^{k} I_{nn}(k) I_{nn}^{T}(k) \tag{9}$$

where H is the size of the moving estimation window:

$$S(k) = C(k)P^{-}(k)C^{T}(k) + V(k) \tag{10}$$

and

$$\delta(k) = \hat{C}_{Inn}(k) - S(k) \tag{11}$$

A positive value of $\delta(k)$ suggests a decrease in the value of **V** and vice versa. In other words, the change of magnitude (positive or negative) of **V** is proportional to the magnitude of $\delta(k)$. Soft computing techniques such as fuzzy logic can be conveniently programmed to this logic. A generic fuzzy rule of the kind

$$IF \ \langle antecedent \rangle \ THEN \ \langle consequent \rangle \tag{12}$$

can be employed for this kind of adaptation behaviour. The antecedent and consequent are of the form $\mathbf{X} \in M_i$, $\mathbf{Y} \in N_i$, $i = 1, 2, \ldots$ respectively where **X** and **Y** represent the input and output variables respectively and M_i and N_i are the fuzzy sets.

Herein, the following three fuzzy rules similar to (12) are used to implement the above covariance matching technique:

IF $\langle \delta(k) \approx 0 \rangle$ THEN $\langle \mathbf{V}(k)$ is unchanged$\rangle$

IF $\langle \delta(k) > 0 \rangle$ THEN $\langle \mathbf{V}(k)$ is decreased$\rangle$

IF $\langle \delta(k) < 0 \rangle$ THEN $\langle \mathbf{V}(k)$ is increased$\rangle$

Thus **V** is adjusted according to

$$\mathbf{V}(k) = \mathbf{V}(k-1) + \Delta\mathbf{V}(k) \tag{13}$$

where $\Delta\mathbf{V}(k)$ is added or subtracted from **V** at each instant of time. Here $\delta(k)$ is the input to the fuzzy inference system (FIS) and $\Delta\mathbf{V}(k)$ is the output.

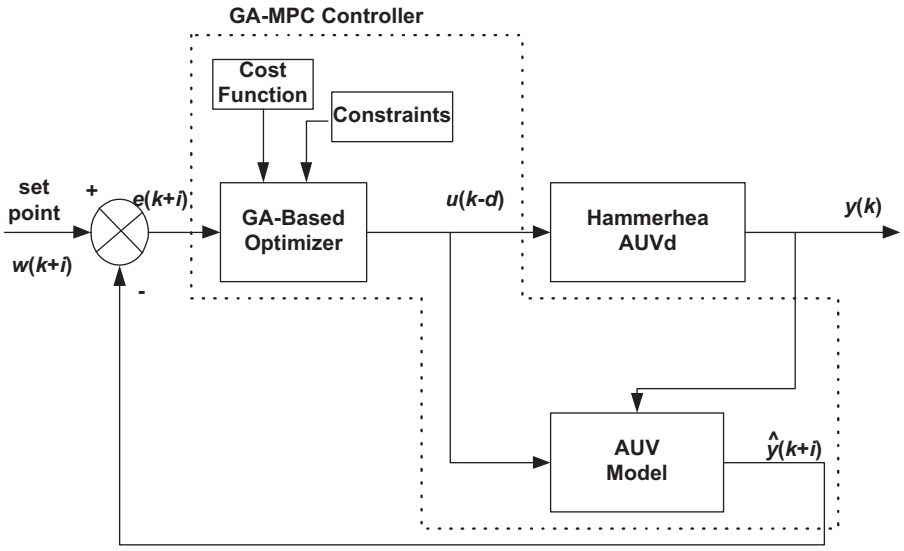

Fig. 5. GA-MPC controller block diagram.

4.2. GA-MPC autopilot design

Model predictive control (MPC), developed by Richalet et al. (1978) of Shell Oil Company in 1978, has been a very successful alternative to PID controllers especially in the petrochemical industry. Several variations of the standard algorithm have since been proposed such as generalised predictive control ((Clarke et al., 1987a,b) and dynamic matrix control (Cutler and Ramaker, 1980). These approaches mainly differ in the plant model integrated within the feedback loop. Since MPC is based on optimal control theory, various optimisation tools have been used to tune the controller online such as quadratic programming, particle swarm optimisation and GAs.

In this paper, a GA has been employed to optimise the performance index in an MPC framework as shown in Fig. 5. This work has been carried out earlier and implemented on the *Hammerhead* AUV (Naeem et al., 2004). The intention here is to compare the performances of both fuzzy-LQG and GA-MPC controllers with feedback obtained from the fuzzy navigation system which is explained in the following section.

5. Sensor data fusion for navigation

Navigation is the science of determining accurately the position and velocity of a dynamic vehicle relative to a reference frame. It serves as an input to the guidance subsystem which plans and executes the manoeuvres necessary to move between the desired locations. A fully autonomous navigation system allows a vehicle to move to a desired destination or along a desired path purposefully without human intervention. Its responsibility is to gather information from every available source (sensors) where each sensor offers its own distinguished outputs to provide a navigation solution. In many applications, more than one sensor is involved so as not only to determine the navigation states at a certain time but also to supply a continuous navigation trajectory. This should also be true in the event of a sensor failure. The term 'multi-sensor navigation system' is therefore often used. Such systems are typically operated with multiple sensors referenced to a common platform and synchronised to a common time base.

Having multiple motion sensors is a necessity for reliable autonomous navigation. In real situations, there is always the potential of sensor failure which could either be temporary or permanent. Hence, to realise reliable and robust navigation in any autonomous vehicle, fault detection and isolation are the main concerns. In any of the sensor fault situations, the navigation system must immediately identify the failed sensor(s) and act in such a way so that erroneous data do not corrupt the global estimates. A simple line of action could be to completely isolate the concerned sensor from the list of active sensors as soon as possible. However, determining the state of a sensor and its isolation in a seamless manner is not trivial and require careful real-time data analysis.

Owing to the potentiality to deal with complex problems, fuzzy logic adaptive (FLA) MSDF techniques have become one of the most popular approaches for multi-sensor navigation. The key advantage fuzzy logic offers the direct representation of the uncertainty in sensor readings in the fusion process by allowing each time-stamped data to be assigned a real number to indicate its degree of truth. In the literature, three main Kalman filter based MSDF architectures have been suggested (Gao and Abousalem, 1993): centralised Kalman filtering (CKF), decentralised Kalman filtering (DKF) and federated Kalman filtering (FKF). All the systems have their own advantages and drawbacks, however, FKF has been recognised as the best solution for fault detection and tolerance (Escamilla-Ambrosio and Mort, 2004). Utilising this knowledge, a modified FLA federated Kalman filter (FKF)-based MSDF architecture was proposed in Naeem et al. (2008) to realise fault-tolerant multi-sensor navigation for *Springer*.

The FLA-FKF, as shown in Fig. 6, is a two-stage data-processing technique which divides the standard Kalman filter into n local filters and a single master filter where n is the number of sensors. In the first stage, all local filters simultaneously analyse and process their own data to yield the best possible local estimate. This is carried out in a similar manner to the adaptive Kalman filter design of the fuzzy LQG autopilot. In the second phase, the feedback factors $\beta(i)$ are determined from the master filter to each local filter. The $\beta(i)$ magnitudes depend on the accuracy of each local filter estimate and hence must be generated online. This means that the most accurate local filter receives the highest feedback from the master filter and thus makes the biggest contribution in the global estimation process. Having done that, the master filter fuses all the local estimates to generate the best global solution. See Appendix B for the FLA-FKF equations.

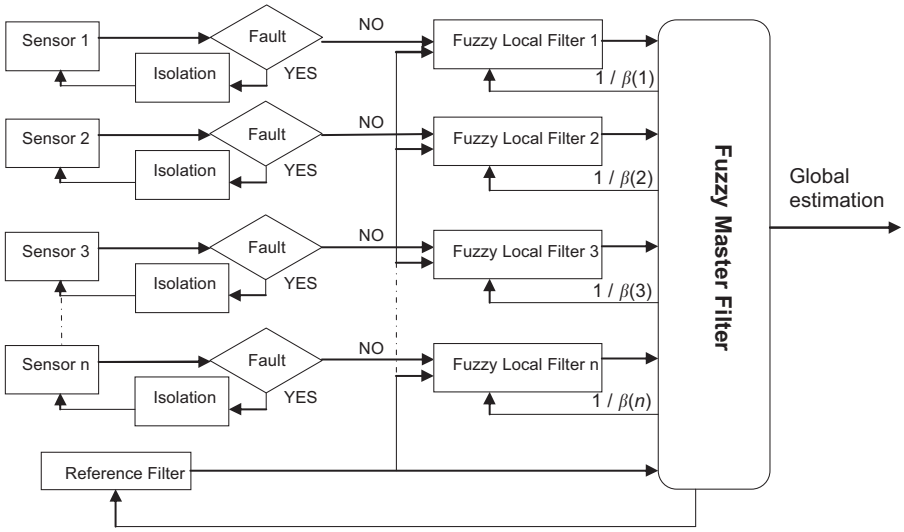

Fig. 6. Fuzzy logic adaptive federated Kalman filter-based MSDF strategy with fault tolerant feature.

6. Experimental design

As mentioned earlier, the SI experiments were conducted by installing an umbilical on the USV which was later removed for full scale control trials. An *ad hoc* wireless network was established, with a maximum range of 500 m, between the vessel and a laptop on a support boat which provides external intervention capabilities for either obstacle avoidance or simply for resetting the system. For waypoint guidance, locations or waypoints were marked prior to the mission using a hand held GPS. For visual confirmation of the target acquisition, buoys already present on the lake were used as targets. A circle of acceptance of radius 10 m was also assumed around each waypoint which signifies the arrival of the vehicle at the target to the mission control software. In addition, a hand held anemometer was also made available to record the wind speed. The guidance algorithms were mainly based on the LOS strategy whereby a LOS angle is calculated between vehicle's current position (measured using an onboard GPS) and the next waypoint. The heading error was recorded with respect to the fused output of the onboard compasses. It should be highlighted that all the experiments were closely monitored from a support boat through a wireless link by constantly following the USV.

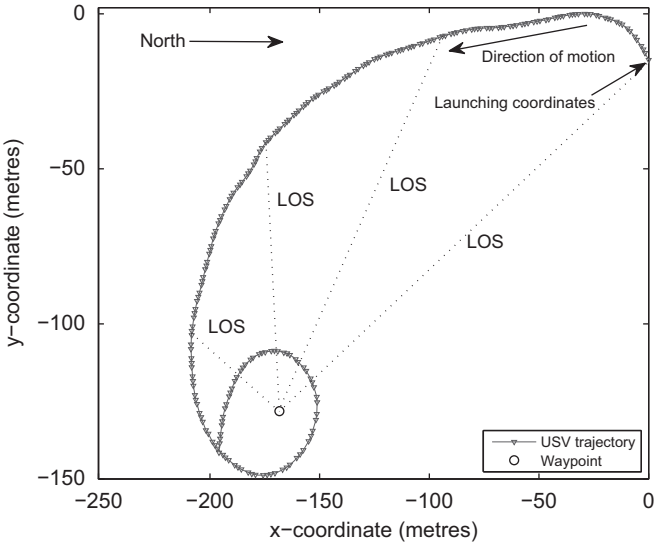

Fig. 7. GA-MPC autopilot performance for waypoint following showing vehicle's trajectory.

7. Results

Initially, all the autopilots designed for the *Springer* were experimented for different mission scenarios including waypoint following, heading regulation and a time-varying reference bearing. Since the GA-MPC was experimented earlier in an AUV, therefore it made sense to test this autopilot first on *Springer* USV to ensure the proper operation of all onboard systems. The mission objective was to arrive at a waypoint by tracking the LOS angle formed between the USV current and waypoint position coordinates. Fig. 7 depicts the vehicle's trajectory transformed from global to body-fixed coordinates. The vessel was at $(-20, 0)$ m with an initial orientation of approximately -150° whereas the waypoint was located at $(-168, -128)$ m; n_d being constrained to ± 500 rpm for all the experiments. A comparison of vehicle's path with the measured LOS angles at various locations shown on the figure demonstrates that the vehicle is struggling to cope with the continuously changing setpoint trajectory. This had resulted due to the slightly heavy weighting of the control term and also due to a mild South-Westerly wind. The measured and desired headings also drifted apart because of this as shown in Fig. 8. Nevertheless, this experiment clearly demonstrated the concept in addition to testing the onboard systems including the wireless link.

For a standard LQG controller, a time-varying heading angle between 200° and 250° was programmed in the mission control software. The vehicle initial orientation was approximately 340° whereas the constraint on n_d was ± 500 rpm as mentioned earlier. Fig. 9 presents both the desired and measured heading angles. Clearly, the vehicle was able to closely follow the trajectory with less than 10% overshoot. The differential input, n_d, also attained the steady state value of zero with small variations to accommodate the required changes in the desired heading and to compensate for external disturbances.

A constant heading following mission was selected to evaluate the performance of the fuzzy-LQG autopilot. The setpoint was chosen as 260° with the vessel pointing at approximately 210° when launched. The control trial result is depicted in Fig. 10. In contrast to the LQG performance, there was no overshoot in this case and the vehicle stayed on course throughout the experiment.

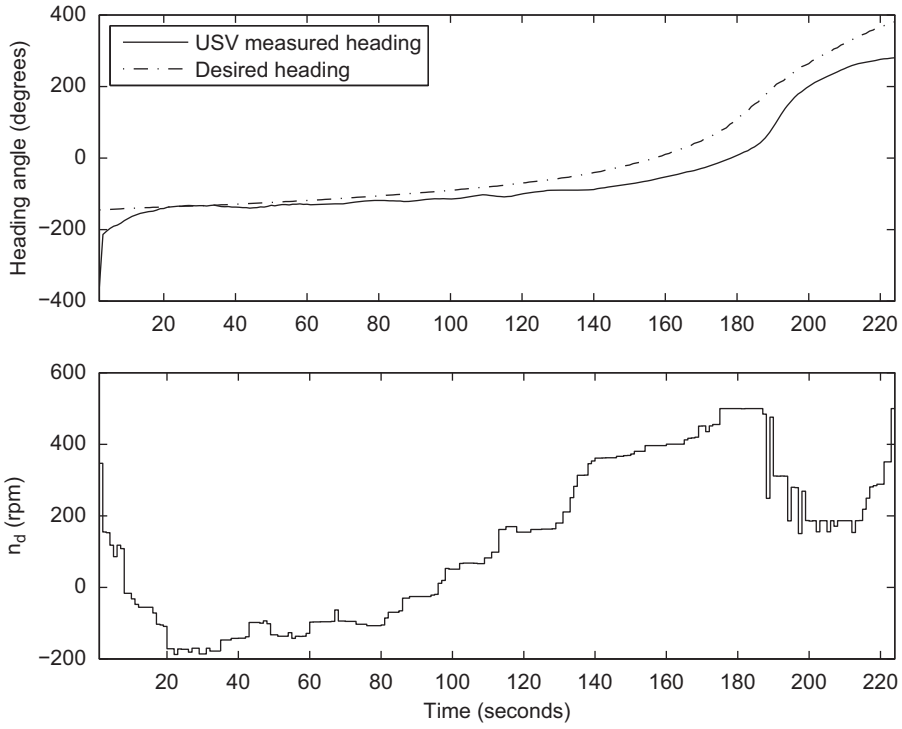

Fig. 8. GA-MPC performance for waypoint following showing heading angle (top) and differential rpm (bottom).

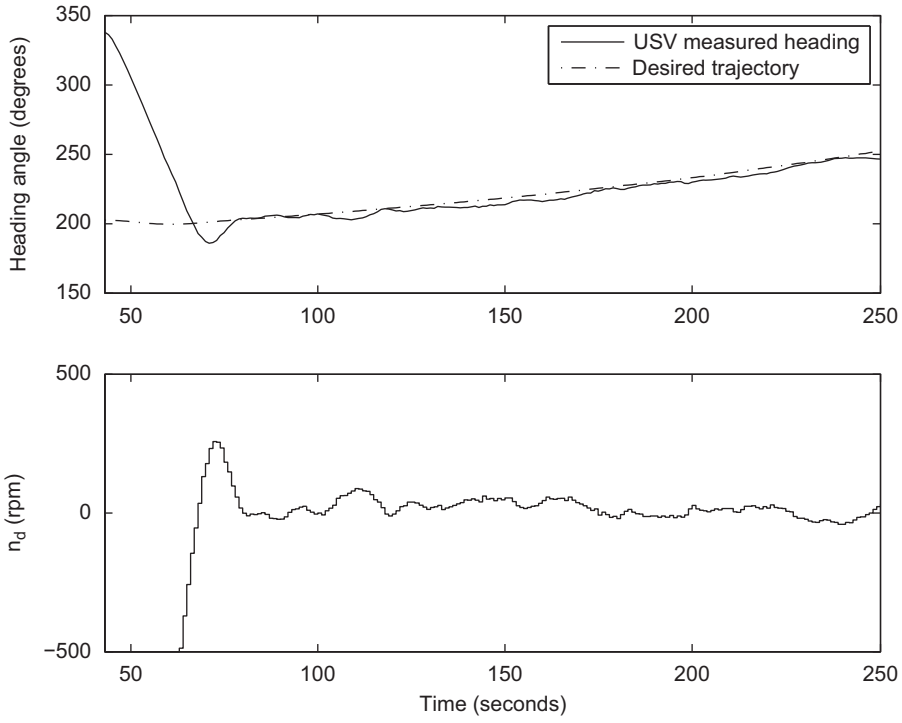

Fig. 9. Standard LQG performance for a time-varying desired heading angle.

The differential input, n_d, was also settled to its steady-state value of zero as illustrated in Fig. 10.

Although the controllers performed reasonably well during the experiments, it was difficult to compare them, hence a single extended waypoint following scenario was chosen so that all the performances can be evaluated. For this purpose, four different waypoints were marked approximately quarter of a km apart from each other and the vehicle was allowed to run between them utilising a different autopilot each time. During the experiments, it was found difficult to maintain the initial position and orientation of the vessel as it drifts because of wind[2] and surface currents. Hence these initial parameters appeared different for

[2] An easterly wind was recorded measured at around 25 km/h using a hand held anemometer.

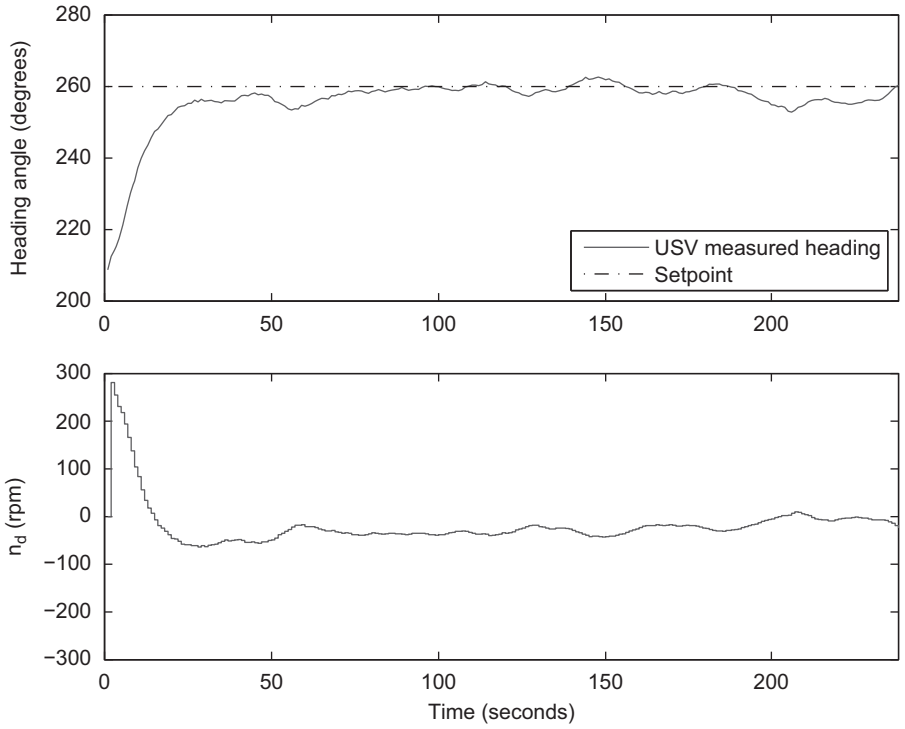

Fig. 10. Fuzzy-LQG performance for a constant heading angle.

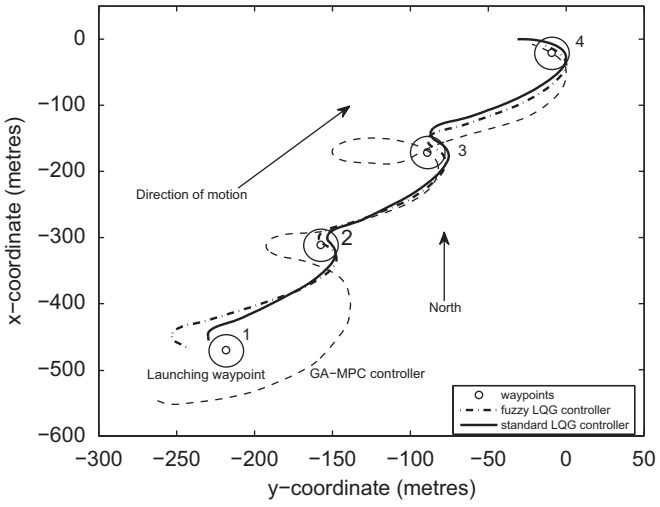

Fig. 11. Waypoint tracking performance comparison.

each controller run. The result is depicted in Fig. 11 for all the cases. Clearly, GA-MPC is the worst contender amongst all of them. Although it managed to track all the waypoints, the performance is rather inadequate with waste of control energy and time. For the second waypoint, the vehicle appears to pass just outside the circle of acceptance and hence could not be declared by the mission control as arrived. Hence a sharp turning manoeuvre was required to achieve that waypoint and to proceed to waypoint 3. On the other hand, the LQG and fuzzy-LQG controllers managed to reach all waypoints almost entirely in straight line manoeuvres. It can be observed from the launching position and orientation of the USV that the convergence rate of fuzzy-LQG is faster than that of its standard counterpart.

Fig. 12 depicts the controller performances in terms of amount of control effort. Both LQG versions have similar control characteristics with the fuzzy-LQG saturates slightly longer to make a sharp turn and take the shortest route.

8. Conclusion

The paper demonstrates the application of advanced navigation, guidance and control algorithms on the *Springer* uninhabited surface vessel. The navigation is based on a fault-tolerant fuzzy logic-based federated Kalman filter multi-sensor data fusion methodology which provides global estimates of the current true state of the vehicle. In this method, the measurement noise covariance matrix of the Kalman filter is manipulated to generate accurate state estimates. The fuzzy LQG autopilot also employs a similar methodology to adapt the Kalman filter for precise state predictions. Both strategies have been combined and experimented in the USV yielding promising results. Standard LQG and GA-MPC controllers were also implemented for several mission scenarios. It was shown that the MSDF strategy provides reliable estimates of the true state of the system. In addition, of the three autopilots tested, the fuzzy LQG was found to deliver the best performance.

As mentioned in the paper, there is currently no obstacle detection and avoidance system onboard the *Springer*, hence constant human supervision is required for proper and safe operation of the craft. Having said that, there are only a handful unmanned marine systems with such a capability. Furthermore, in order to be able to integrate these USVs into the ambient marine traffic, they must adhere to the same navigation regulations as any manned vehicle would follow, i.e. marine 'rules of the road' defined by the international maritime organisation. Current projects (Zolfagharifard, 2010) are investigating into this by developing a reliable collision detection and avoidance module to be integrated so that complete autonomy could be achieved.

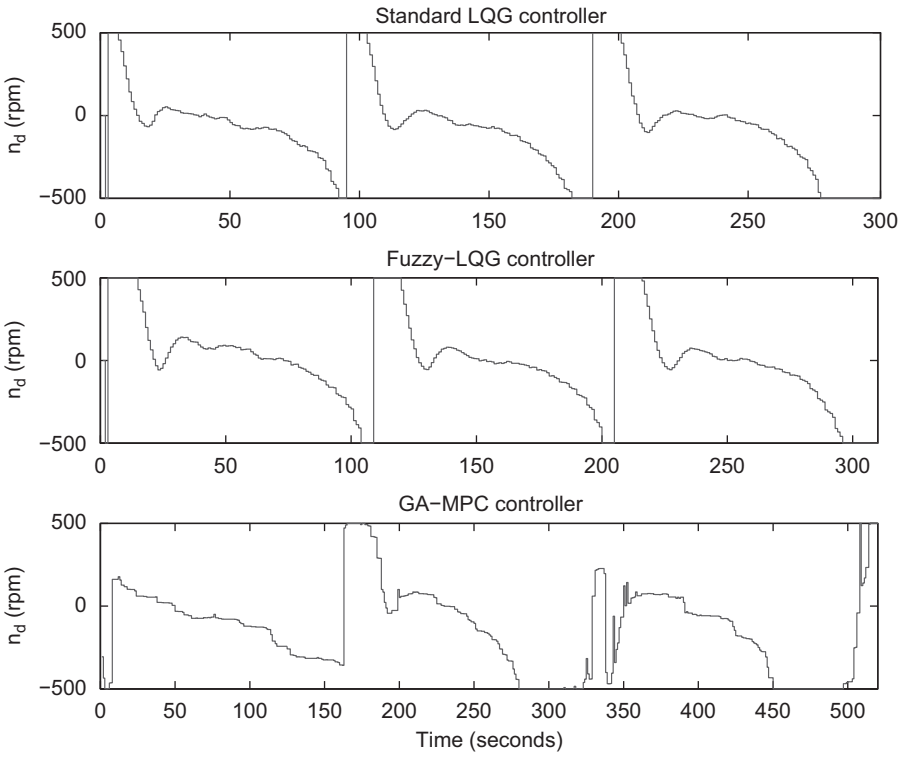

Fig. 12. Waypoint tracking performance, differential input.

Acknowledgments

The authors would like to thank the Engineering and Physical Sciences Research Council, UK for the funding of this project.

Appendix A. LQG standard equations

Consider a discrete linear time invariant system represented in state-space form as follows:

$$\mathbf{x}(k+1)=\mathbf{A}\mathbf{x}(k)+\mathbf{B}u(k)$$

$$y(k)=\mathbf{C}\mathbf{x}(k)+\mathbf{D}u(k)$$

The control law is given by

$$u=-\mathbf{K}_c\hat{x}(k)$$

where $\hat{x}$ is the estimated state and u is the control action. The combination of LQR and Kalman filter will result in the following optimal state-feedback controller given by

$$\hat{x}(k+1)=(\mathbf{A}-\mathbf{B}\mathbf{K}_c-\mathbf{K}_f\mathbf{C}\mathbf{A}+\mathbf{K}_f\mathbf{C}\mathbf{B}\mathbf{K}_c)\hat{x}(k)+(\mathbf{A}-\mathbf{B}\mathbf{K}_c)\mathbf{K}_f\mathbf{e}(k)$$

$$u(k)=\mathbf{K}_c(\mathbf{I}-\mathbf{K}_f\mathbf{C})\hat{x}(k)+\mathbf{K}_c\mathbf{K}_f\mathbf{e}(k)$$

where $\mathbf{e}=\mathbf{r}-\hat{x}$ is the error between a reference vector $\mathbf{r}$ and plant states $\hat{x}$.

Appendix B. Fuzzy logic adaptive federated Kalman filter equations

A typical procedure for a FKF can be described mathematically as follows:

$$\mathbf{W}_i(k)=(1/\beta_i)\mathbf{W}_f(k) \tag{B.1}$$

$$\mathbf{P}_i^+(k)=(1/\beta_i)\mathbf{P}_f^+(k) \tag{B.2}$$

$$\hat{x}_i^+(k)=(1/\beta_i)\hat{x}_f^+(k) \tag{B.3}$$

where $\mathbf{W}$ is the process noise covariance matrix and i is the index of n local Kalman filters. In the local Kalman filters:

$$\hat{x}_i^+(k)=\hat{x}_f^+(k) \tag{B.4}$$

subject to

$$\sum_{i=1}^{n}\beta_i=1 \tag{B.5}$$

$$\hat{x}_i^-(k+1)=\mathbf{A}_i(k+1)\hat{x}_i^+(k)+\mathbf{B}_i(k)u_i(k) \tag{B.6}$$

$$\mathbf{P}_i^-(k+1)=\mathbf{A}_i(k)\mathbf{P}_i^+(k)\mathbf{A}_i^T(k)+\mathbf{W}_i(k) \tag{B.7}$$

$$\mathbf{K}_i(k)=\mathbf{P}_i^-(k)\mathbf{C}_i^T(k)+[\mathbf{C}_i(k)\mathbf{P}_i^-(k)\mathbf{C}_i^T(k)+\mathbf{V}_i(k)]^{-1} \tag{B.8}$$

$$\hat{x}_i^+(k)=\hat{x}_i^-(k)+\mathbf{K}_i(k)[z_i(k)-\mathbf{C}_i(k)\hat{x}_i^-(k)] \tag{B.9}$$

$$\mathbf{P}_i^+(k)=[I-\mathbf{K}_i(k)\mathbf{C}_i(k)]\mathbf{P}_i^{-1}(k)[I-\mathbf{K}_i(k)\mathbf{C}_i(k)]^T+\mathbf{K}_i(k)\mathbf{V}_i(k)\mathbf{K}_i^T(k) \tag{B.10}$$

For the master filter:

$$\hat{x}_M^-(k+1)=\mathbf{A}_M(k+1)\hat{x}_M^+(k)+\mathbf{B}_M(k)u_M(k) \tag{B.11}$$

$$\mathbf{P}_M^-(k+1)=\mathbf{A}_M(k)\mathbf{P}_M^+(k)\mathbf{A}_M^T(k)+\mathbf{W}_M(k) \tag{B.12}$$

The global estimate is then calculated as follows:

$$\mathbf{P}_f^+(k)^{-1}=\sum_{i=1}^{n}[\mathbf{P}_i^+(k)]^{-1}-[\mathbf{P}_M^-(k)]^{-1} \tag{B.13}$$

$$\hat{x}_f^+(k)=\mathbf{P}_f^+(k)\left[\mathbf{P}_M^-(k)^{-1}\hat{x}_i^-(k)+\sum_{i=1}^{n}\mathbf{P}_i^+(k)^{-1}\hat{x}_i^+(k)\right] \tag{B.14}$$

where $\mathbf{P}_f^+(k)$ is the inverse of $\mathbf{P}_f^+(k)^{-1}$

The information feedback factors are calculated according to the following equation (Xu et al., 2006):

$$\beta_i = \frac{\mathrm{tr}\,\Lambda_i'}{\sum_{j=1}^{m} \mathrm{tr}\,\Lambda_j'} \tag{B.15}$$

where $\Lambda_i' = diag(\lambda_{i1}', \lambda_{i2}', \ldots, \lambda_{iN}')$ are the eigenvalues of P_i.

B.1. Nomenclature

m	mass of the vehicle
p	angular velocity along the x-axis
r	angular velocity along the z-axis
u	surge velocity
v	sway velocity
x_G	x-coordinate of the centre of gravity
y_G	y-coordinate of the centre of gravity
I_x	moment of inertia about the x-axis
I_{xy}	product of inertia about x- and y-axes
X,Y,Z	external forces along the x-, y- and z-axes
K,M,N	external moments along the x-, y- and z-axes
K_c,K_f	LQR and Kalman filter gains
$\hat{A}$	predicted value of an arbitrary state A

References

Clarke, D.W., Mohtadi, C., Tuffs, P.S., 1987a. Generalized predictive control: I. The basic algorithm. Automatica 23 (2), 137.

Clarke, D.W., Mohtadi, C., Tuffs, P.S., 1987b. Generalized predictive control: II. Extensions and interpretations. Automatica 23 (2), 149.

Cutler, C.R., Ramaker, B.L., 1980. Dynamic matrix control—a computer control algorithm, paper wp5-b. In: Proceedings of the Joint Automatic Control Conference, San Francisco, CA.

Escamilla-Ambrosio, P.J., Mort, N., 2004. Comparison of three fuzzy logic-based adaptive multi-sensor data fusion architecture. In: Proceedings of the 3rd IFAC Symposium on Mechatronic Systems, IFAC, pp. 10–108.

Fossen, T.I., 1994. Guidance and Control of Ocean Vehicles. John Wiley & Sons Ltd.

Gao, Y.K., Abousalem, M.A., 1993. Comparison and analysis of centralized, decentralized, and federated filters. J. Inst. Navig. 40 (1), 69–86.

Jordan, K., 2008. Remus AUV Plays Key Role in Iraq War 〈http://www.hydroidinc.com/〉. World Wide Web, Date Accessed, May 18th, 2011.

Loebis, D., Sutton, R., Chudley, J., 2004a. A fuzzy Kalman filter optimized using a multiobjective genetic algorithm for enhanced autonomous underwater vehicle navigation. Proc. Inst. Mech. Eng. (IMechE) Part M 218 (1), 53–69.

Loebis, D., Sutton, R., Chudley, J., Naeem, W., 2004b. Adaptive tuning of a Kalman filter via fuzzy logic for an intelligent AUV navigation system. Control Eng. Pract. 12 (12), 1531–1539.

Maridan, A., 2008. AUV Technology 〈http://www.maridan.atlas-elektronik.com/〉. World Wide Web, Date Accessed, May 18th, 2011.

Mehra, R., 1970. On the identification of variances and adaptive Kalman filtering. IEEE Trans. Autom. Control 15 (2), 175–184.

Naeem, W., Sutton, R., Chudley, J., 2006. Soft computing design of a linear quadratic Gaussian controller for an unmanned surface vehicle. In: 14th IEEE Mediterranean Conference on Control and Automation, June. IEEE, Ancona, Italy.

Naeem, W., Sutton, R., Chudley, J., 2007. Chemical plume tracing and odour source localisation by autonomous vehicles. J. Navig. 60 (2), 173–190.

Naeem, W., Sutton, R., Chudley, J., Dalgleish, F.R., Tetlow, S., 2004. An online genetic algorithm based model predictive control autopilot design with experimental verification. Int. J. Control 78 (14), 1076–1090.

Naeem, W., Xu, T., Sutton, R., Tiano, A., 2008. The design of a navigation guidance and control system for an unmanned surface vehicle for environmental monitoring. IMeChE Trans. Part M, J. Eng. Marit. Environ. 222 (2), 67–79 (Special issue on Marine Systems).

Pascoal, A., Oliveira, P., Silvestre, C., Sebastiao, L., Rufino, M., Barroso, V., Gomes, J., Ayela, G., Coince, P., Cardew, M., Ryan, A., Braithwaite, H., Cardew, N., Trepte, J., Seube, N., Champeau, J., Dhaussy, P., Sauce, V., Moitie, R., Santos, R., Cardigos, F., Brussienx, M., Dando, P., 2000. Robotic ocean vehicles for marine science applications: the European ASIMOV project. Oceans 2000 MTS/IEEE Conference and Exhibition, September, vol. 1. IEEE/MTS, Providence, RI, pp. 409–415.

Petroleum, B., 2010. Gulf of Mexico Response 〈http://www.bp.com/sectionbodycopy.do?categoryId=41&contentId=7067505〉. World Wide Web, Date Accessed, May 18th, 2011.

Richalet, J.A., Rault, A., Testud, J.D., Papon, J., 1978. Model predictive heuristic control: applications to industrial processes. Automatica 14, 413–428.

Roboteq, I., 2010. Roboteq ax2550/2850 user's manual 〈http://www.roboteq.com〉. World Wide Web, Date Accessed, May 18th, 2011.

Shao, Z.J., Wang, H., Zhu, Y.K., Qian, J.X., 1994. Multivariable optimal control with adaptation mechanism in rudder/fin stabilizing system. In: Proceedings of the IEEE International Conference on Industrial Technology. IEEE, December, pp. 53–57.

Xu, T., Chudley, J., Sutton, R., 2006. A fault tolerant multi-sensor navigation system for an unmanned surface vehicle. In: Proceedings of 6th IFAC Symposium on Fault Detection, Supervision and Safety of Technical Processes, IFAC, Tsinghua University, China, August/September.

Zolfagharifard, E., 2010. EPSRC Funds USV Collision Avoidance System 〈http://www.theengineer.co.uk/news/epsrc-funds-usv-collision-avoidance-system/1004270.article〉. World Wide Web, Date Accessed, May 18th, 2011.